Free vibration analysis of FG nanoplates using quasi-3D hyperbolic refined plate theory and the isogeometric approach

Amir Farzam[1,*], Behrooz Hassani[2,*], Abbas Karamodin[1]

1. Department of Civil Engineering, Ferdowsi University of Mashhad, Iran
am_fa110@yahoo.com & a-karam@um.ac.ir
2. Department of Mechanical Engineering, Ferdowsi University of Mashhad, Iran
b_hassani@um.ac.ir

Abstract

In this paper, quasi three-dimensional (quasi-3D) hyperbolic shear deformation theory is used for the free vibration analysis of functionally graded nanoplates by using the isogeometric analysis (IGA) approach and nonlocal elasticity theory. The quasi-3D theory using five independent unknowns satisfies the free transverse shear stress conditions on the top and bottom surfaces of plate and so a shear correction factor is not needed. The displacement field takes into account both shear deformation and thickness stretching effect and the equations are derived based on physical neutral surface position. The IGA approach can easily formulate C^1 continuous elements by using Non-Uniform Rational B-Spline (NURBS) functions. Numerical results are compared with other solutions.

Keywords: Free vibration analysis, Functionally graded materials, Isogeometric approach, Nonlocal elasticity theory, Quasi-3D hyperbolic refined plate theory.

1. Introduction

In recent years, many research studies have been carried out to predict the behavior of nanostructures. The continuum mechanics approach which provides more simplicity and efficiency than molecular dynamics approach, is widely used to study the mechanical behavior of nanostructures. The local (classical) continuum theories do not model the behavior of nanoscale structures properly. In order to consider small scale effects in nanoscale structures, different size-dependent continuum mechanics models have been developed such as the couple stress theory [1,2], gradient theory [3], nonlocal elasticity theory [4-6], strain gradient theory [7,8], modified couple stress theory [9], modified strain gradient theory [10] and surface energy theory [11]. Many publications show that the nonlocal elasticity theory considering small scale effects can well predict the behavior of nanostructures. Aghababaei and Reddy [12] used third order shear deformation plate theory for the bending and vibration of nanoplates. Ansari and et al. [13] presented nonlocal plate model for the free vibration of single-layered graphene sheets. Malekzadeh and et al. [14] utilized nonlocal elasticity theory for the free vibration of orthotropic nanoplates. Jomehzadeh and Saidi [15] presented the three dimensional vibration analysis of nanoplates. Hosseini-Hashemi and et al. [16] presented an exact analytical approach for the free vibration of Mindlin rectangular nanoplates. Daneshmehr et al. [17] utilized nonlocal elasticity theory for the free vibration analysis of nanoplates. Sarrami-Foroushani and Azhari [18] used finite strip method to analyze the rectangular nanoplates based on refined plate theory. Ansari and et al. [19] presented the three dimensional vibration analysis of nanoplates on elastic foundations. Ilkhani et al. [20] used wave propagation approach for the free vibration of thin rectangular nanoplates. Most of the studies in functionally graded (FG) nanoplates are based on the classical and first order shear deformation theories and a few studies are available using other shear deformation theories.

To analyze plate structures, many theories have been presented. The classical plate theory (CPT) gives acceptable results for thin plates. The first order shear deformation theory (FSDT) which accounts for transverse shear deformation effects, requires a shear correction factor to satisfy the free transverse shear stress conditions on the top and bottom surfaces of plate. To avoid the use of shear correction factor, many higher order shear deformation theories (HOSDT) have been proposed such as third order shear deformation theory (TSDT) [21], sinusoidal shear deformation theory (SSDT) [22,23], hyperbolic shear deformation theory (HSDT) [24-31] and so on [32]. In order to reduce the number of unknowns in HOSDT, the refined plate theory (RPT) model was proposed by Senthilnathan et al. [33]. The RPT divides transverse displacement into bending and shear components and by making further assumptions, decreases the number of unknowns in displacement field.

There are several numerical methods to solve problems. Hughes et al. [34] introduced isogeometric analysis (IGA) approach which represents the exact geometry of problem by the use of Non-Uniform Rational B- Spline (NURBS). The IGA approach can easily form C^1 continuous elements by using B-splines or NURBS approximations. However the IGA approach has been widely used to analyze various problems, there are only a few studies which analyze nanostructures. Natarajan et al. [35] presented the free vibration analysis of functionally graded nanoplates based on FSDT. Nguyena et al. [36] utilized the IGA approach to analyze functionally graded nanoplates.

In this paper quasi-3D hyperbolic shear deformation theory is used for the free vibration analysis of functionally graded nanoplates by using the IGA approach and nonlocal elasticity theory based on physical neutral surface position. The following section presents the equations of nonlocal elasticity theory. In section 3 quasi-3D hyperbolic shear deformation theory is introduced for FG nanoplates based on physical neutral surface position. In section 4, the equations of nanoplate theory is provided based on NURBS basis functions. In section 5, numerical results and discussions are provided. Finally, this paper is closed by conclusions.

2. Nonlocal elasticity theory

According to the nonlocal elasticity theory, the stress at a reference point x is a function of strain field at every point in the body. The stress is defined as [4-5]

$$(1-\mu\nabla^2)\sigma_{ij}^{nl}=\sigma_{ij}^{l} \tag{1a}$$

$$\mu=(e_0 a)^2 \tag{1b}$$

$$\nabla^2=\frac{\partial^2}{\partial x^2}+\frac{\partial^2}{\partial y^2} \tag{1c}$$

Here, σ_{ij}^{nl} and σ_{ij}^{l} are nonlocal and local stress respectively. μ is nonlocal parameter which represents the small scale effect. e_0 is a constant determined for each material type and a is an internal characteristics length.

3. Quasi-3D refined plate theory for FG nanoplates

1-3- Physical neutral surface

The neutral surface position of FG plates may not coincide with its middle surface due to the lack of symmetry. If the origin of the coordinate system is located on the neutral surface position, FG plates can be easily analyzed with the isotropic plate theories. z_{ms} and z_{ns} planes are considered to determine the neutral surface position of FG plates as shown in Fig. 1.

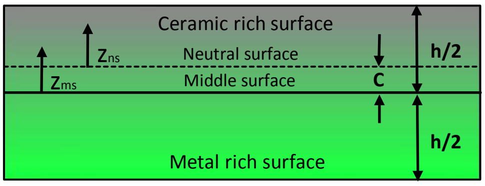

Fig. 1: Geometry of functionally graded plates.

Consider a FG rectangular plate with length a, width b and constant thickness h. The position of the neutral surface (C) can be calculated by the use of the equilibrium equation as

$$C=\frac{\int_{-h/2}^{h/2} E(z_{ms})z_{ms}dz_{ms}}{\int_{-h/2}^{h/2} E(z_{ms})dz_{ms}} \tag{2}$$

The nonhomogeneous properties of materials may be obtained by means of the rule of mixture. The volume fraction of ceramic V_C in the new coordinate system can be expressed as

$$V_C=(\frac{z_{ms}}{h}+\frac{1}{2})^k=(\frac{z_{ns}+C}{h}+\frac{1}{2})^k \tag{3}$$

where the power k is greater than or equal to zero. The Young's modulus of FG plate is a function of the thickness coordinate as follows

$$E(z_{ns})=E_m+(E_c-E_m)\left(\frac{z_{ns}+C}{h}+\frac{1}{2}\right)^k \tag{4}$$

For Mori–Tanaka scheme, the Young's modulus is given as [37,38]

$$E(z_{ns}) = E_m + (E_c - E_m)\frac{V_C}{1 + V_m(\frac{E_c}{E_m} - 1)(\frac{1+\nu}{3-3\nu})}, \quad V_m = V_C - 1 \tag{5}$$

2-3- Quasi-3D RPT based on physical neutral surface

Based on the RPT, the displacements of a material point located at (x, y, z) in a plate may be written as

$$\begin{aligned} u(x,y,z_{ns}) &= u_0 - z_{ns}\frac{\partial w_b}{\partial x} + g(z_{ns})\frac{\partial w_s}{\partial x} \\ v(x,y,z_{ns}) &= v_0 - z_{ns}\frac{\partial w_b}{\partial y} + g(z_{ns})\frac{\partial w_s}{\partial y} \\ w(x,y,z_{ns}) &= w_b + w_s + \Psi'(z_{ns})\beta \end{aligned} \tag{6}$$

where u, v, w are displacements in the x, y, z directions, u_0, v_0, w_b and w_s are mid-plane, bending and shear deflections and β is the rotation of the xy plane due to shear. The function $g(z_{ns}) = \Psi(z_{ns}) - (z_{ns} + C)$ is used to describe the distribution of transverse shear strains and stresses through the plate thickness. In this paper $\Psi(z_{ns})$ function is presented as [32]:

$$\Psi(z_{ns}) = ((z_{ns} + C)/h)(cosh(0.5) + 0.5sinh(0.5) - cosh((z_{ns} + C)/h)) \tag{7}$$

The relationships between strains and displacements are described as

$$\{\varepsilon\} = \begin{Bmatrix} \varepsilon_x \\ \varepsilon_y \\ \gamma_{xy} \end{Bmatrix} = \begin{Bmatrix} \varepsilon_x^0 \\ \varepsilon_y^0 \\ \gamma_{xy}^0 \end{Bmatrix} + z_{ns}\begin{Bmatrix} k_x^b \\ k_y^b \\ k_{xy}^b \end{Bmatrix} + g(z_{ns})\begin{Bmatrix} k_x^s \\ k_y^s \\ k_{xy}^s \end{Bmatrix} \tag{8}$$

$$\{\gamma\} = \begin{Bmatrix} \gamma_{xz} \\ \gamma_{yz} \end{Bmatrix} = \Psi'(z_{ns})\begin{Bmatrix} \gamma_{xz}^s \\ \gamma_{yz}^s \end{Bmatrix}$$

$$\{\varepsilon_z\} = \Psi''(z_{ns})\beta$$

where

$$\begin{Bmatrix} \varepsilon_x^0 \\ \varepsilon_y^0 \\ \gamma_{xy}^0 \end{Bmatrix} = \begin{Bmatrix} \frac{\partial u_0}{\partial x} \\ \frac{\partial v_0}{\partial y} \\ \frac{\partial u_0}{\partial y} + \frac{\partial v_0}{\partial x} \end{Bmatrix}, \begin{Bmatrix} k_x^b \\ k_y^b \\ k_{xy}^b \end{Bmatrix} = -\begin{Bmatrix} \frac{\partial^2 w_b}{\partial x^2} \\ \frac{\partial^2 w_b}{\partial y^2} \\ 2\frac{\partial^2 w_b}{\partial x \partial y} \end{Bmatrix}, \begin{Bmatrix} k_x^s \\ k_y^s \\ k_{xy}^s \end{Bmatrix} = \begin{Bmatrix} \frac{\partial^2 w_s}{\partial x^2} \\ \frac{\partial^2 w_s}{\partial y^2} \\ 2\frac{\partial^2 w_s}{\partial x \partial y} \end{Bmatrix}, \begin{Bmatrix} \gamma_{xz}^s \\ \gamma_{yz}^s \end{Bmatrix} = \begin{bmatrix} \frac{\partial w_s}{\partial x} + \frac{\partial \beta}{\partial x} \\ \frac{\partial w_s}{\partial y} + \frac{\partial \beta}{\partial x} \end{bmatrix} \tag{9}$$

Based on the Hooke's law the stresses are written as

$$(1 - \mu\nabla^2)\begin{Bmatrix} \sigma_x \\ \sigma_y \\ \sigma_z \\ \tau_{xy} \\ \tau_{xz} \\ \tau_{yz} \end{Bmatrix} = \begin{bmatrix} C_{11} & C_{12} & C_{13} & 0 & 0 & 0 \\ C_{12} & C_{22} & C_{23} & 0 & 0 & 0 \\ C_{13} & C_{23} & C_{33} & 0 & 0 & 0 \\ 0 & 0 & 0 & C_{44} & 0 & 0 \\ 0 & 0 & 0 & 0 & C_{55} & 0 \\ 0 & 0 & 0 & 0 & 0 & C_{66} \end{bmatrix}\begin{Bmatrix} \varepsilon_x \\ \varepsilon_y \\ \varepsilon_z \\ \gamma_{xy} \\ \gamma_{xz} \\ \gamma_{yz} \end{Bmatrix} \tag{10}$$

$$C_{11} = C_{22} = C_{33} = \frac{(1-\nu)E(z_{ns})}{(1-2\nu)(1+\nu)}$$

$$C_{12}=C_{13}=C_{23}=\frac{\nu E(z_{ns})}{(1-2\nu)(1+\nu)}$$
$$C_{44}=C_{55}=C_{66}=\frac{E(z_{ns})}{2(1+\nu)}$$

The total potential energy can be given as

$$\Pi=U-T \tag{11}$$

where U, and T are strain energy, and kinetic energy.
The strain energy is defined as

$$U=\frac{1}{2}\iint_{-\frac{h}{2}-C}^{\frac{h}{2}-C}\sigma\,\varepsilon dV=\frac{1}{2}\iint_{-\frac{h}{2}-C}^{\frac{h}{2}-C}(\sigma_x^{nl}\varepsilon_x+\sigma_y^{nl}\varepsilon_y+\sigma_z^{nl}\varepsilon_z+\tau_{xy}^{nl}\gamma_{xy}+\tau_{xz}^{nl}\gamma_{xz}+\tau_{zy}^{nl}\gamma_{zy})\,dz_{ns}dA \tag{12}$$

By substituting Eq. (8) into Eq. (12), the potential energy of the plate is rewritten as

$$U=\frac{1}{2}\int(N_x\varepsilon_x^0+N_y\varepsilon_y^0+N_{xy}\gamma_{xy}^0+M_x^bk_x^b+M_y^bk_y^b+M_{xy}^bk_{xy}^b+M_x^sk_x^s+M_y^sk_y^s+M_{xy}^sk_{xy}^s+S_{xz}^s\gamma_{xz}^s+S_{yz}^s\gamma_{yz}^s+R_z\beta)\,dA \tag{13}$$

where the stress resultants N, M, S and R are defined as

$$\left(N_x,N_y,N_{xy}\right)=\int_{-\frac{h}{2}-C}^{\frac{h}{2}-C}(\sigma_x,\sigma_y,\tau_{xy})^{(nl)}dz_{ns} \tag{14a}$$
$$(M_x^b,M_y^b,M_{xy}^b)=\int_{-\frac{h}{2}-C}^{\frac{h}{2}-C}(\sigma_x,\sigma_y,\tau_{xy})^{(nl)}z_{ns}dz_{ns} \tag{14b}$$
$$\left(M_x^s,M_y^s,M_{xy}^s\right)=\int_{-\frac{h}{2}-C}^{\frac{h}{2}-C}(\sigma_x,\sigma_y,\tau_{xy})^{(nl)}g(z_{ns})dz_{ns} \tag{14c}$$
$$(S_{xz}^s,S_{yz}^s)=\int_{-\frac{h}{2}-C}^{\frac{h}{2}-C}(\tau_{xz,}\tau_{yz,})^{(nl)}\Psi'(z_{ns})dz_{ns} \tag{14d}$$
$$R_z=\int_{-\frac{h}{2}-C}^{\frac{h}{2}-C}\sigma_z{}^{(nl)}\Psi''(z_{ns})dz_{ns} \tag{14e}$$

By substituting Eq. (9) into Eq. (10) and the subsequent results into Eqs. (14a-e), the stress resultants are obtained as

$$(1-\mu\nabla^2)\begin{Bmatrix}\{N\}\\\{M^b\}\\\{M^s\}\\\{R_z\}\end{Bmatrix}=[D^b]\begin{Bmatrix}\{\varepsilon^0\}\\\{k^b\}\\\{k^s\}\\\{\beta\}\end{Bmatrix} \tag{15a}$$
$$(1-\mu\nabla^2)\{S^s\}=[D^s]\{\gamma^s\} \tag{15b}$$

where the material matrices are given as

$$[D^b]=\begin{bmatrix}[A] & [B] & [D] & [G_1]^T\\ [B] & [C] & [E] & [G_2]^T\\ [D] & [E] & [F] & [G_3]^T\\ [G_1] & [G_2] & [G_3] & [G_4]\end{bmatrix} \tag{16}$$

$$([A],[B],[C],[D],[E],[F]) = \begin{bmatrix}1 & \nu & 0\\ \nu & 1 & 0\\ 0 & 0 & \frac{1-\nu}{2}\end{bmatrix}\int_{-\frac{h}{2}-C}^{\frac{h}{2}-C}(1,z_{ns},z_{ns}^2,g(z_{ns}),z_{ns}g(z_{ns}),g^2(z_{ns}))\frac{E(z_{ns})}{1-\nu^2}\,dz_{ns}$$

$$([G_1],[G_2],[G_3]) = [1 \quad 1 \quad 0]\int_{-\frac{h}{2}-C}^{\frac{h}{2}-C}\frac{\nu E(z_{ns})}{(1-2\nu)(1+\nu)}(1,z_{ns},g(z_{ns}))\Psi''(z_{ns})dz_{ns}$$

$$[G_4]=\int_{-\frac{h}{2}-C}^{\frac{h}{2}-C}\frac{(1-\nu)E(z_{ns})}{(1-2\nu)(1+\nu)}(\Psi''(z_{ns}))^2dz_{ns}$$

$$[D^s]=\begin{bmatrix}1 & 0\\ 0 & 1\end{bmatrix}\int_{-\frac{h}{2}-C}^{\frac{h}{2}-C}\frac{E(z_{ns})}{2(1+\nu)}(\Psi'(z_{ns}))^2dz_{ns}$$

The kinetic energy and its variation is obtained as

$$\mathrm{T}=\frac{1}{2}\int \rho\,[(\dot{u})^2+(\dot{v})^2+(\dot{w})^2]dV \tag{17}$$

$$\delta\mathrm{T}=\iint_{-\frac{h}{2}-C}^{\frac{h}{2}-C}(\dot{u}\delta\dot{u}+\dot{v}\delta\dot{v}+\dot{w}\delta\dot{w})\rho(\mathrm{z_{ns}})d\mathrm{z_{ns}}dA=-\int(\delta\{\tilde{u}\}^T-\mu\nabla^2\delta\{\tilde{u}\}^T)\,[m]\{\ddot{\tilde{u}}\}dV \tag{18}$$

where m is the mass matrix defined as

$$[m]=\begin{bmatrix}I_0 & 0 & 0\\ 0 & I_0 & 0\\ 0 & 0 & I_{00}\end{bmatrix}, I_0=\begin{bmatrix}I_1 & I_2 & I_4\\ I_2 & I_3 & I_5\\ I_4 & I_5 & I_6\end{bmatrix}, I_{00}=\begin{bmatrix}I_1 & I_7 & I_4\\ I_7 & I_8 & I_5\\ I_4 & I_5 & I_6\end{bmatrix} \tag{19}$$

$$(\mathrm{I_1,I_2,I_3,I_4,I_5,I_6,I_7,I_8}) = \int_{-\frac{\mathrm{h}}{2}-\mathrm{C}}^{\frac{\mathrm{h}}{2}-\mathrm{C}}(1,\mathrm{z_{ns}},\mathrm{z_{ns}}^2,\mathrm{g(z_{ns})},\mathrm{z_{ns}g(z_{ns})},\mathrm{g^2(z_{ns})},\Psi'(\mathrm{z_{ns}}),(\Psi'(\mathrm{z_{ns}}))^2)\rho(\mathrm{z_{ns}})d\mathrm{z_{ns}}$$

$$\{\tilde{u}\}=\{u_0,-\frac{\partial w_b}{\partial x},\frac{\partial w_s}{\partial x},v_0,-\frac{\partial w_b}{\partial y},\frac{\partial w_s}{\partial y},(w_b+w_s),\beta,0\}^T \tag{20}$$

4. FG nanoplate formulation based on NURBS basis functions

1-4- NURBS functions

A non-decreasing knot vector in the parametric space [34] is define as

$$U=\{u_0,u_1,u_2,\dots,u_m\},\ u_i\le u_{i+1},\ i=0,1,2,3,\dots,m-1 \qquad m=n+p+1 \tag{21}$$

Here u_i are the *i-th* knot, *p* is the polynomial degree and *n+1* is the number of basis functions. The knots equally spaced in the parametric space are said to be uniform knots. A knot vector the first and the last knots are repeated $p+1$ times, is said to be open knot vector and is defined as

$$U = \left\{ \underbrace{a, \cdots, a}_{p+1}, u_{m-p-1}, \underbrace{b, \cdots, b}_{p+1} \right\} \tag{22}$$

The B-spline basis functions of degree *p*, are defined as

$$N_{i,0}(u) = \begin{cases} 1 & if\ u_i \le u \le u_{i+1} \\ 0 & \text{otherwise} \end{cases} \tag{23}$$

$$N_{i,p}(u) = \frac{u - u_i}{u_{i+p} - u_i} N_{i,p-1}(u) + \frac{u_{i+p+1-u}}{u_{i+p+1} - u_{i+1}} N_{i+1,p-1}(u)$$

A piecewise-polynomial B-spline curve is defined as

$$C(u) = \sum_{i=0}^{n} N_{i,p}(u) \times P_i \ , \quad \mathrm{a} \le \mathrm{u} \le \mathrm{b} \tag{24}$$

where $\{p_i\}$ are the control points and $\{N_{i,p}(u)\}$ are the B-spline basis functions of degree *p*. Similarly, a B-spline surface of degree *p*, is defined as

$$S(u, v) = \sum_{i=0}^{n} \sum_{j=0}^{m} N_{i,p}(u) N_{j,q}(v) P_{i,j} \tag{25}$$

Where $\{P_{i,j}\}$ form a bidirectional control net, $\{N_{i,p}(u)\}$ and $\{N_{j,q}(v)\}$ are the B-spline basis functions defined on the knot vectors as

$$U = \left\{ \underbrace{0, \ldots., 0}_{p+1}, u_{p+1}, \ldots., u_{r-p-1}, \underbrace{1, \ldots., 1}_{p+1} \right\} \tag{26}$$

$$V = \left\{ \underbrace{0, \ldots., 0}_{q+1}, v_{q+1}, \ldots., v_{s-q-1}, \underbrace{1, \ldots., 1}_{q+1} \right\}$$

NURBS curve and surface of degree *p* are defined as

$$C(u) = \frac{\sum_{i=0}^{n} N_{i,p}\,(u) w_i P_i}{\sum_{i=0}^{n} N_{i,p}\,(u) w_i} \tag{27}$$

$$S_{i,j}(u, v) = \frac{\sum_{i=0}^{n} \sum_{j=0}^{m} N_{i,p}(u)\, N_{j,q}\,(v) w_{i,j} P_{i,j}}{\sum_{i=0}^{n} \sum_{j=0}^{m} N_{i,p}(u)\, N_{j,q}\,(v) w_{i,j}} \tag{28}$$

where $\{w_i\}$ are the weights.

Rational B-spline basis function and NURBS surface defined in Eq. (28), can be expressed as

$$R_{i,j}(u,v) = \frac{N_{i,p}(u)N_{j,q}(v)w_{i,j}}{\sum_{k=0}^{n}\sum_{l=0}^{m} N_{k,p}(u)\, N_{l,q}\,(v)w_{k,l}} \tag{29}$$

$$S(u,v) = \sum_{i=0}^{n}\sum_{j=0}^{m} R_{i,j}(u,v)P_{i,j} \tag{30}$$

2-4- Quasi-3D RPT formulation based on NURBS approximations

The variation of strain energy can be written as

$$\delta U = \int \delta\,\{\varepsilon\}^{T}[\bar{D}]\{\varepsilon\}dV \tag{31}$$

The global stiffness matrix K is computed as

$$[K] = \int([B^{m}]^{T}\,[D^{b}][B^{m}] + [B^{s}]^{T}[D^{s}][B^{s}])d\Omega \tag{32}$$

where

$$[B_i^{m}] = \begin{bmatrix} R_{i,x} & 0 & R_{i,y} & 0 & 0 & 0 & 0 & 0 & 0 & 0 \\ 0 & R_{i,y} & R_{i,x} & 0 & 0 & 0 & 0 & 0 & 0 & 0 \\ 0 & 0 & 0 & -R_{i,xx} & -R_{i,yy} & -2R_{i,xy} & 0 & 0 & 0 & 0 \\ 0 & 0 & 0 & 0 & 0 & 0 & R_{i,xx} & R_{i,yy} & 2R_{i,xy} & 0 \\ 0 & 0 & 0 & 0 & 0 & 0 & 0 & 0 & 0 & R_i \end{bmatrix}^{T} \tag{33}$$

$$[B_i^{s}] = \begin{bmatrix} 0 & 0 & 0 & R_{i,x} & R_{i,x} \\ 0 & 0 & 0 & R_{i,y} & R_{i,y} \end{bmatrix}$$

The Hamilton's principle is used to derive the equation of the free vibration analysis as

$$\delta\int_0^t (T-U)dt = \int_0^t (\delta T - \delta U)dt = 0 \;\; \Rightarrow \int \delta\,\{\varepsilon\}^{T}[\bar{D}]\{\varepsilon\}\mathrm{dV} = -\int \delta\,\{\tilde{u}\}^{T}[m]\{\ddot{\tilde{u}}\}\mathrm{dV} \tag{34}$$

The Eq. (34) can be simplified as

$$([\mathrm{K}] - \omega^{2}[\mathrm{M}])\{\mathrm{D}\} = 0 \tag{35}$$

where

$$[M] = \int ([\tilde{R}]^{T} - \mu\nabla^{2}[\tilde{R}]^{T})[m][\tilde{R}]d\Omega$$

$$[\tilde{R}] = \begin{bmatrix} R_i & 0 & 0 & 0 & 0 & 0 & 0 & 0 & 0 \\ 0 & 0 & 0 & R_i & 0 & 0 & 0 & 0 & 0 \\ 0 & -R_{i,x} & 0 & 0 & -R_{i,y} & 0 & R_i & 0 & 0 \\ 0 & 0 & R_{i,x} & 0 & 0 & R_{i,y} & R_i & 0 & 0 \\ 0 & 0 & 0 & 0 & 0 & 0 & 0 & R_i & 0 \end{bmatrix}^{T}$$

5. Results and discussions

In this section the results of the free vibration analysis of FG nanoplates are presented. First the convergence of results for natural frequencies are examined. Then the efficiency of the present model is shown by comparing the obtained results with 3D solutions based on local elasticity theory (μ = 0). Finally, the results are presented for FG and isotropic nanoplates. To obtain results, (p+1)×(q+1) Gauss points are utilized. The material properties of FG nanoplates are listed in Table 1. Different boundary conditions are considered including simply supported:

$$v_0 = w_b = w_s = 0 \quad \text{at } x = 0, a \qquad (36)$$
$$u_0 = w_b = w_s = 0 \quad \text{at } y = 0, b$$

Clamped:

$$u_0 = v_0 = w_b = w_s = \beta = w_{b,n} = w_{s,n} = \beta_{,n} = 0 \qquad (37)$$

Table 1: Material properties of FG nanoplates.

Material	E (GPa)	ρ (kg/m^3)	ν
SUS304	201.04	8166	0.3
Si_3N_4	348.43	2370	0.3

1-5- Convergence study

Consider an isotropic square plate with fully simply supported boundary conditions. The convergence of non-dimensional natural frequencies for a/h = 10 and μ = 0 is shown in Table 2 based on quartic NURBS elements (p = 4). However a mesh of 5×5 is enough for fundamental frequency but it is not enough for higher order frequencies. In other words, higher order frequencies are more sensitive to meshes in comparison with lower order frequencies. So in this paper a mesh of 11×11 quartic NURBS elements are used to solve problems as shown in Fig. 3.

Table 2: Convergence of the non-dimensional natural frequencies $\bar{\omega} = \omega(a^2/\pi^2)\sqrt{\rho h/G}$ of SSSS isotropic square plates (a/h = 10).

Mode	Meshes						3D [39]
	3×3	5×5	7×7	9×9	11×11	13×13	
1	1.9343	1.9342	1.9342	1.9342	1.9342	1.9342	1.9342
2	4.6379	4.6225	4.6222	4.6222	4.6222	4.6222	4.6222
3	4.6379	4.6225	4.6222	4.6222	4.6222	4.6222	4.6222
4	6.5234	6.5234	6.5234	6.5234	6.5234	6.5234	6.5234
5	6.5234	6.5234	6.5234	6.5234	6.5234	6.5234	6.5234
6	7.1247	7.1035	7.1032	7.1032	7.1032	7.1032	7.1030
7	8.6664	8.6776	8.6633	8.6623	8.6622	8.6621	8.6617
8	8.6664	8.6776	8.6633	8.6623	8.6622	8.6621	8.6617

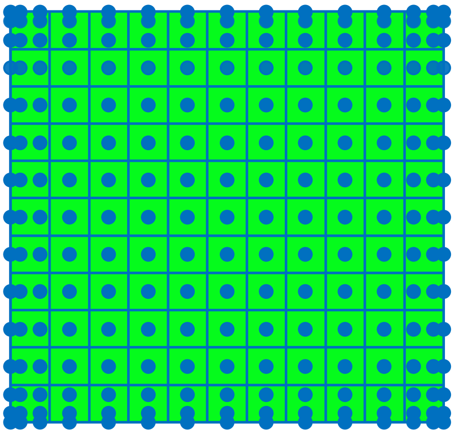

Fig. 3: Square plate: meshing of 11×11 quartic elements.

2-5- Free vibration analysis

Table 3 presents the non-dimensional fundamental frequency of SSSS isotropic rectangular nanoplates by assuming a = 10, E = 30×10^6 and ν = 0.3. The results are compared with the solutions of 3D (Ansari et al. [19] and Jomehzadeh et al. [15]), CPT, FSDT and TSDT (Aghababaei and Reddy [12]). Furthermore in Table 4, the results are presented for different boundary conditions for square nanoplates. As observed in Table 4, CCCC boundary condition gives higher values for frequency in comparison with SSSS.

Table 3: Non-dimensional fundamental frequency $\bar{\omega} = \omega h\sqrt{\rho/G}$ of SSSS isotropic nanoplates (a = 10, E = 30×10^6, ν = 0.3).

a/b	a/h	μ	3D [15,19]	CPT [12]	FSDT [12]	TSDT [12]	Present
1	10	0	0.0931	0.0963	0.0930	0.0935	0.0932
		1	0.0827	0.0880	0.0850	0.0854	0.0851
		2	0.0751	0.0816	0.0788	0.0791	0.0789
		3	0.0692	0.0763	0.0737	0.0741	0.0738
		4	0.0646	0.0720	0.0696	0.0699	0.0696
	20	0	0.0239	0.0241	0.0239	0.0239	0.0239
		1	0.0211	0.0220	0.0218	0.0218	0.0218
		2	0.0191	0.0204	0.0202	0.0202	0.0202
		3	0.0176	0.0191	0.0189	0.0189	0.0189
		4	0.0164	0.0180	0.0178	0.0179	0.0178
2	10	0	-	0.0602	0.0589	0.0591	0.0589
		1	-	0.0568	0.0556	0.0557	0.0556
		2	-	0.0539	0.0527	0.0529	0.0528
		3	-	0.0514	0.0503	0.0505	0.0503
		4	-	0.0493	0.0482	0.0483	0.0482
	20	0	-	0.0150	0.0150	0.0150	0.0150
		1	-	0.0142	0.0141	0.0141	0.0141
		2	-	0.0135	0.0134	0.0134	0.0134
		3	-	0.0129	0.0128	0.0128	0.0128
		4	-	0.0123	0.0123	0.0123	0.0122

Table 4: Non-dimensional fundamental frequency $\bar{\omega} = \omega h\sqrt{\rho/G}$ of isotropic square nanoplates (a = 10, a/h = 10, E = 30×10^6, ν = 0.3).

μ	SSSC	SCSC	CCCS	CCCC
0	0.1110	0.1345	0.1467	0.1636
1	0.1009	0.1218	0.1321	0.1469
2	0.0930	0.1120	0.1211	0.1344
3	0.0868	0.1043	0.1124	0.1245
4	0.0816	0.0980	0.1053	0.1165

In Fig. 4, the effect of the parameters a/h, μ, and *k* on the fundamental frequency of SSSS FG nanoplates are depicted. As depicted in Fig. 4, the frequency decreases by increasing the nonlocal parameter μ, length–thickness ratio a/h, aspect ratio b/a and power index *k*.

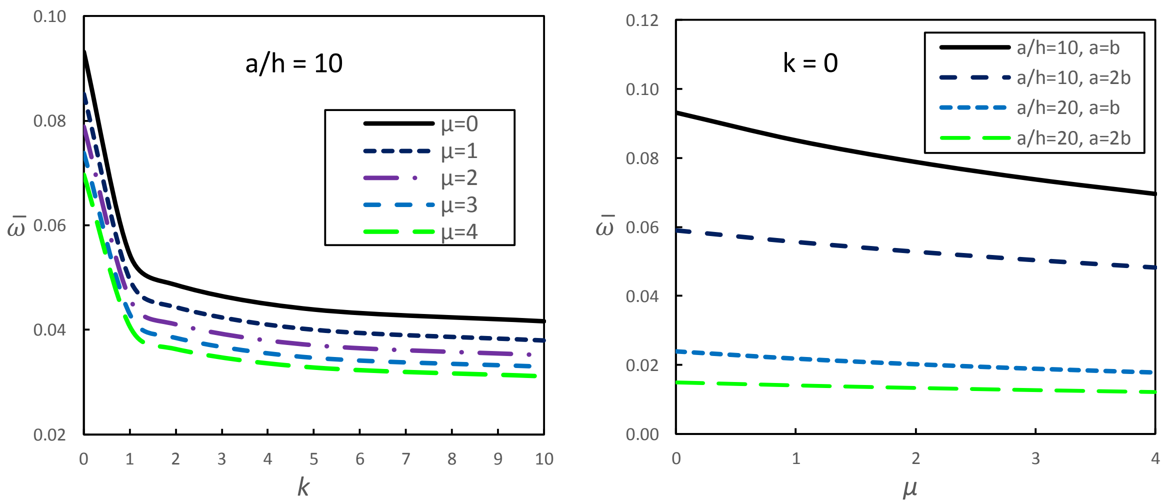

Fig. 4: Effect of the parameters a/h, μ, and *k* on the fundamental frequency of SSSS SUS304/Si3N4 nanoplates.

Table 5: Non-dimensional natural frequencies $\bar{\omega} = \omega h\sqrt{\rho_c/G_c}$ of SSSS SUS304/Si_3N_4 square nanoplates (a = 10, a/h = 10).

k	Model	Mode 1				Mode 2			
		μ				μ			
		0	1	2	4	0	1	2	4
1	Present	0.0543	0.0496	0.0460	0.0406	0.1297	0.1061	0.0920	0.0752
	Nguyena et al. [36]	0.0538	0.0491	0.0455	0.0402	0.1259	0.1031	0.0894	0.0730
2	Present	0.0486	0.0444	0.0411	0.0363	0.1158	0.0947	0.0821	0.0671
	Nguyena et al. [36]	0.0480	0.0439	0.0406	0.0359	0.1122	0.0918	0.0796	0.0651
5	Present	0.0438	0.0401	0.0371	0.0328	0.1044	0.0854	0.0741	0.0605
	Nguyena et al. [36]	0.0433	0.0396	0.0367	0.0324	0.1010	0.0827	0.0717	0.0586
	Natarajan et al. [35]	0.0441	0.0403	0.0374	0.0330	0.1051	0.0860	0.0746	0.0610
10	Present	0.0416	0.0380	0.0352	0.0311	0.0991	0.0811	0.0703	0.0575
	Nguyena et al. [36]	0.0411	0.0375	0.0348	0.0307	0.0959	0.0785	0.0680	0.0556

In Table 5 the non-dimensional natural frequencies of SSSS SUS304/Si_3N_4 square nanoplates are given for different power indices *k* and nonlocal parameter μ. The length a = 10 and length–thickness a/h = 10 are assumed. It is seen that the results are close to the solution of Nguyena et al. [36]. In Table 6, the results are also presented for CCCC boundary condition.

Table 6: Non-dimensional natural frequencies $\bar{\omega} = \omega h\sqrt{\rho_c/G_c}$ of CCCC SUS304/Si_3N_4 square nanoplates (a = 10, a/h = 10).

k	Mode 1				Mode 2			
	μ				μ			
	0	1	2	4	0	1	2	4
0	0.1636	0.1469	0.1344	0.1165	0.3160	0.2519	0.2154	0.1734
1	0.0954	0.0857	0.0783	0.0679	0.1841	0.1467	0.1254	0.1009
2	0.0851	0.0764	0.0699	0.0606	0.1639	0.1307	0.1117	0.0899
5	0.0766	0.0688	0.0630	0.0546	0.1475	0.1176	0.1006	0.0810
10	0.0728	0.0654	0.0598	0.0518	0.1401	0.1118	0.0956	0.0770

6. Conclusions

In this paper, quasi-3D hyperbolic shear deformation theory has been presented to analyze FG nanoplates by using the IGA approach and nonlocal elasticity theory based on physical neutral surface position. The principles of Hamilton is utilized to derive the equations. The theory uses five independent unknowns and satisfies the free transverse shear stress conditions on the top and bottom surfaces of the plate without a need for shear correction factor. It is observed that, the natural frequencies decrease by increasing the nonlocal parameter μ, length–thickness ratio a/h, aspect ratio b/a and power index *k*. It is also seen that higher order frequencies are more sensitive to the number of meshes in comparison with lower order frequencies. The present results can be utilized as benchmark solutions for future researches.

References

[1] Toupin RA. Theories of elasticity with couple-stress. Archive for Rational Mechanics and Analysis, 1964;17:85–112.

[2] Mindlin RD, Tiersten HF. Effects of couple-stresses in linear elasticity. Archive for Rational Mechanics and Analysis, 1962;11:415–48.

[3] Mindlin RD. Second gradient of strain and surface tension in linear elasticity. International Journal of Solids and Structures, 1965;1:417–38.

[4] Eringen AC. Nonlocal polar elastic continua. International Journal of Engineering Science, 1972;10:1–16.

[5] Eringen AC. On differential equations of nonlocal elasticity and solutions of screw dislocation and surface waves. Journal of Applied Physics, 1983;54:4703–10.

[6] Eringen AC, Edelen DGB. On nonlocal elasticity. International Journal of Engineering Science, 1972;10:233–48.

[7] Fleck NA, Hutchinson JW. A phenomenological theory for strain gradient effects in plasticity. Journal of the Mechanics and Physics of Solids, 1993;41:1825–57.

[8] Altan BS, Aifantis EC. On the structure of the mode III crack-tip in gradient elasticity. Scripta Metallurgica Materialia, 1992;26:319–24.

[9] Yang F, Chong ACM, Lam DCC, Tong P. Couple stress based strain gradient theory for elasticity. International Journal of Solids and Structures, 2002;39:2731–43.

[10] Lam DCC, Yang F, Chong ACM, Wang J, Tong P. Experiments and theory in strain gradient elasticity. Journal of the Mechanics and Physics of Solids, 2003;51:1477–508.

[11] Dingreville Rm, Qu J, Cherkaoui M. Surface free energy and its effect on the elastic behavior of nano sized particles, wires and films. Journal of the Mechanics and Physics of Solids, 2005;53:1827–54.

[12] Aghababaei R, Reddy JN. Nonlocal third-order shear deformation plate theory with application to bending and vibration of plates. Journal of Sound and Vibration, 2009;326:277–89.

[13] Ansari R, Sahmani S, Arash B. Nonlocal plate model for free vibrations of single-layered graphene sheets. Physics Letters A, 2010;375:53–62.

[14] Malekzadeh P, Setoodeh AR, Alibeygi Beni A. Small scale effect on the free vibration of orthotropic arbitrary straight-sided quadrilateral nanoplates. Composite Structures, 2011;93:1631–39.

[15] Jomehzadeh E, Saidi AR. Decoupling the nonlocal elasticity equations for three dimensional vibration analysis of nano-plates. Composite Structures, 2011;93:1015–20.

[16] Hosseini-Hashemi S, Zare M, Nazemnezhad R. An exact analytical approach for free vibration of Mindlin rectangular nano-plates via nonlocal elasticity. Composite Structures, 2013;100:290–99.

[17] Daneshmehr A, Rajabpoor A, Hadi A. Size dependent free vibration analysis of nanoplates made of functionally graded materials based on nonlocal elasticity theory with high order theories. International Journal of Engineering Science, 2015;95:23–35.

[18] Sarrami-Foroushani S, Azhari M. Nonlocal buckling and vibration analysis of thick rectangular nanoplates using finite strip method based on refined plate theory. Acta Mechanica, 2016;227:721–42.

[19] Ansari R, Shahabodini A, Faghih Shojaei M. Nonlocal three-dimensional theory of elasticity with application to free vibration of functionally graded nanoplates on elastic foundations. Physica E, 2016;76:70–81.

[20] Ilkhani MR, Bahrami A, Hosseini-Hashemi SH. Free vibrations of thin rectangular nano-plates using wave propagation approach. Applied Mathematical Modelling, 2016;40:1287–99.

[21] Reddy JN. A simple higher-order theory for laminated composite plates. Journal of Applied Mechanics, 1984;51(4):745–52.

[22] Touratier M. An efficient standard plate theory. International Journal of Engineering Science, 1991;29(8):901–16.

[23] Arya H, Shimpi RP, Naik NK. A zigzag model for laminated composite beams. Composite Structures, 2002;56(1):21–4.

[24] Soldatos KP, Timarci T. A unified formulation of laminated composite, shear deformable, five-degrees of-freedom cylindrical shell theories. Composite Structures, 1993;25:165–71.

[25] Akavci SS. Two new hyperbolic shear displacement models for orthotropic laminated composite plates. Mechanics of Composite Materials, 2010;46(2):215–26.

[26] Akavci SS. An efficient shear deformation theory for free vibration of functionally graded thick rectangular plates on elastic foundation. Composite Structures, 2014;108:667–76.

[27] Akavci SS, Tanrikulu AH. Static and free vibration analysis of functionally graded plates based on a new quasi-3D and 2D shear deformation theories. Composites Part B: Engineering, 2015;83:203–15.

[28] Mahi A, Bedia EAA, Tounsi A. A new hyperbolic shear deformation theory for bending and free vibration analysis of isotropic, functionally graded, sandwich and laminated composite plates. Applied Mathematical Modelling, 2015;39:2489–08.

[29] Mechab I, Mechab B, Benaissa S. Static and dynamic analysis of functionally graded plates using four variable refined plate theory by the new function. Composites Part B: Engineering, 2013;45:748–57.

[30] Meiche NE, Tounsi A, Zlane N, Mechab I, Bedia EAA. A new hyperbolic shear deformation theory for buckling and vibration of functionally graded sandwich plate. International Journal of Mechanical Sciences, 2011;53: 237–47.

[31] Farzam-Rad SA, Hassani B, Karamodin A. Isogeometric analysis of functionally graded plates using a new quasi-3D shear deformation theory based on physical neutral surface. Compos Part B, 2017;108:174–89.

[32] Farzam A, Hassani B. A new efficient shear deformation theory for FG plates with in-plane and through-thickness stiffness variations using isogeometric approach. Mechanics of Advanced Materials and Structures, (http://dx.doi.org/10.1080/15376494.2017.1400623).

[33] Senthilnathan NR, Lim SP, Lee KH, Chow ST. Buckling of shear-deformable plates. AIAA Journal, 1987;25(9): 1268–71

[34] Hughes TJR, Cottrell JA, Bazilevs Y. Isogeometric analysis: CAD, finite elements, NURBS, exact geometry and mesh refinement. Computer Methods in Applied Mechanics and Engineering, 2005;194:4135–95.

[35] Natarajan S, Chakraborty S, Thangavel M, Bordas S, Rabczuk T. Size-dependent free flexural vibration behavior of functionally graded nanoplates. Computational Materials Science, 2012;65:74–80.

[36] Nguyena NT, Huic D, Leeb J, Nguyen-Xuand H. An efficient computational approach for size-dependent analysis of functionally graded nanoplates. Computer Methods in Applied Mechanics and Engineering, 2015;297:191–218.

[37] Benveniste Y. A new approach to the application of Mori–Tanaka’s theory in composite materials. Mechanics of Materials, 1987;6:147–57.

[38] Mori T, Tanaka K. Average stress in matrix and average elastic energy of materials with misfitting inclusions. Acta Metallurgica, 1973;21:571–74.

[39] Zhou D, Cheung YK, Au FTK, Lo SH. Three-dimensional vibration analysis of thick rectangular plates using Chebyshev polynomial and Ritz method. International Journal of Solids and Structures, 2002;39(26):6339–53.